Heritage Science

RESEARCH

Open Access

Influence of polar amino acids on the carbonation of lime mortars

Kun Zhang[1], Yufan Zhang[1], Yan Liu[1], Lu Wang[1], Lu He[1], Taoling Dong[1], Ruicong Lu[1], Yue Zhang[2] and Fuwei Yang[1*]

Abstract

The addition of protein-based additives (e.g. milk, egg white, animal blood) into lime mortars can improve mortar properties such as workability, strengths and durability. With the intent to understand how and why proteinaceous additives improve lime mortar properties, it could be useful to start from the basic building blocks of proteins amino acids. Consequently, the present study focuses on the influence of polar amino acids on the carbonation of lime mortars, and the results demonstrated that addition of amino acids into mortars could slow down mortar drying, increase surface hardness, slow down carbonation, promote amorphous calcium carbonate stabilization and inhibit calcite formation; moreover, these effects seemed to become more evident with the increase of amino acid concentration. It was speculated that in highly alkaline lime mortars, polar amino acids could lime carbonation by interacting with calcium carbonate via H-bonds and additional Ca^{2+} mediated adsorption.

Keywords: Lime mortar, Amino acid, Amorphous calcium carbonate, FTIR, XRD, TGA

Introduction

Mortars with proteinaceous additives were traditional construction materials frequently used all around the world, as confirmed by vast amounts of historic literatures. For instance, pig blood, lime and Liaojiang stone powder a pozzolanic material commonly found in northwestern China were said to be used in the foundation of Xianyang Palace (~350 B.C.) in Xi'an, China [1]; the use of bullock's blood, lime and oil/iron dross as remedy mortars to be laid on cracks of baths was accounted in *Opus Agriculturae* (fourth–fifth century A.D.) [2]; egg white and cheese, when mixed together with other additives in lime, can be used as plaster, as described in Corning's version of *Mappae Clavicular* (twelfth century A.D.) [3]; the monk Theophilus Presbyter, writing in his handbook (~1100–1120 A.D.) that, the mixture of small pieces of cheese, quicklime and water can be used as glue for wood panels in church buildings [4]; milk and oil mixed with lime and sand, can consist a mortar for a sun-dial-plane, as mentioned by Richard Neve in his *The City and Country Purchaser's and Builder's Dictionary* (1726 A.D.) [5]; animal glue, linseed oil, and rosin bulked with a calcium filler was used most extensively from the fourth quarter of the eighteenth century to the present to create sculptural relief in architectural interiors and on picture frames [6].

Some previous studies showed that, the addition of protein-based additives such as animal blood, milk, egg white, animal glue, etc. into lime-based mortars can impart them with superior properties in both fresh and hardened state, such as increased workability [7, 8], mortar strengths [9–11], water retaining capacity[9], water resistance [9, 10, 12–14] and frost resistance [9]. Other studies, on the contrary, concluded that proteinaceous addition could have negative effects on mortar properties, such as decreased mortar strengths [7, 8, 13–15] and water resistance [7]. Alonso et al. [15] showed that

*Correspondence: yangfuwei@nwu.edu.cn

[1] China-Central Asia "the Belt and Road" Joint Laboratory On Human and Environment Research, Key Laboratory of Cultural Heritage Research and Conservation, School of Culture Heritage, Northwest University, Xi'an 710127, China
Full list of author information is available at the end of the article

25% milk addition into lime mortar resulted in lower compressive and tensile strengths, while the 50% and 75% addition resulted in higher compressive and tensile strengths than specimen without organic addition. Zhao et al. [16] found that compressive strength of lime mortar was increased by 1% pig blood addition, but greatly decreased by the 3% and 5% addition. Mydin et al. [17] indicated that compressive and flexural strengths of lime mortar increased with 2–6% egg white addition, but decreased with 8% and 10% addition.

No unanimous conclusion can be summarized out of the above studies, on one hand because the natural protein-based additives are mixtures of different types of substances (e.g. proteins, carbohydrates, fats and salts), and components such as carbohydrates and fats could also influence mortar properties. On the other hand, the protein contents in the additives are different, for example, ~ 5% wt. in milk [18], ~ 10% wt. in egg white [19–21], and ~ 20% wt. in animal blood [22], also making it difficult to fairly compare the results among different studies. In addition, proteins are organized in complex primary, secondary, tertiary or quaternary structures, and each level of these structures may exert additional impacts on mortars.

Therefore, it might be useful to start from the basic building blocks of proteins amino acids so that the future studies could move on to higher orders of protein hierarchical structures. An amino acid consists of an alpha carbon, a basic amino group (-NH_2), an acidic carboxyl group (-COOH), and an organic R group (or side chain) that is unique to each amino acid. Amino acids can be classified into polar and nonpolar amino acids, basing upon the polarity of the R group.

It is well-known that polar amino acids (such as serine (Ser) [23–25], cysteine (Cys) [23, 26], asparagine (Asn)/aspartic acid (Asp) [24, 25, 27–29], Glutamine (Gln)/glutamic acid (Glu) [27, 29], and lysine (Lys) [26]) play crucial roles in controlling crystalline forms and morphology of calcium carbonate in the biomineralization process. Consequently, as a first understanding on how and why amino acids influence lime mortar properties, the present study intends to acquire some preliminary results on the effects of polar amino acids on lime carbonation, which was rarely discussed in other studies on mortars. Khan et al. [30] investigated the control of amino acids on $CaCO_3$ crystallization in carbonated cement composites, and found that the addition of amino acids resulted in the formation of stable amorphous calcium carbonate (ACC), vaterite, and aragonite, at the same time increasing flexural and compressive strengths of the composites. The authors assumed that such performance enhancement was attributed to reduced critical pore size and formation of organic–inorganic hybrid phases in the matrix.

The results of the present study could hopefully serve to understand the possible mechanism of traditional mortars with protein additives, at the same time making contribution to the development of restoration materials for historic architectures.

Experimental

Materials

The 11 polar amino acids [L-serine (Ser), L-threonine (Thr), L-cysteine (Cys), L-tyrosine (Tyr), L-asparagine (Asn), L-glutamine (Gln), L-aspartic acid (Asp), L-glutamic acid (Glu), L-lysine (Lys), L-arginine (Arg), and L-histamine (His)] were purchased from Sigma-Aldrich, Germany, and used without further purification. All amino acids were used in biologically relevant L-enantiomers to prevent additional influences caused by chirality [31–34]. Molecular structures of the 11 polar amino acids were produced using a Kingdraw software (Qingyuan Precision Agriculture Technology Co., Ltd., China), as shown in Fig. 1.

The calcium hydroxide used in the present study was an analytical reagent in powder form ($Ca(OH)_2$, 95%, CAS no. 1305-62-0), a commercial product purchased from Sinopharm Chemical Reagent Co. Ltd., China. The mineralogical composition of the calcium hydroxide was analyzed by X-ray diffraction analysis (PANalytical X'pert^3 Powder), the Jade International Center for Diffraction data (ICDD) Powder Diffraction File (PDF) database was used to detect the major presence of portlandite (#44-1481), see Fig. 2.

To provide the mortar with adequate strength for the surface hardness test, sand was also included in the mortar mixes. The sand used in the present study was purchased from Fujian Non-metallic Mineral Co. Ltd., China. The mineral composition and particle size distribution of the sand were characterized, as respectively shown in Fig. 3a, b. The X-ray diffraction analysis (PANalytical X'pert^3 Powder) result showed that the major mineral composition of the sand was quartz (ICDD PDF#46-1045). The particle size distribution analysis (Malvern Mastersizer 2000) result showed that the 10th percentile [d(0.1)], median [d(0.5)] and 90th percentile [d(0.9)] particle size of the sand were 312.82, 486.82 and 700.92 μm, respectively.

Mortar specimen preparation

The 11 polar amino acids (AA) were separately mixed with double-distilled water (W) at percentages of AA/(AA + W) = 5, 10 and 20% by weight. Such 3 percentages were chosen to conform to the protein contents in three of the most commonly used proteinaceous additives in historic mortars: bovine milk (~ 3.5% protein content [18]), egg white (~ 10–13% protein content [19–21]) and

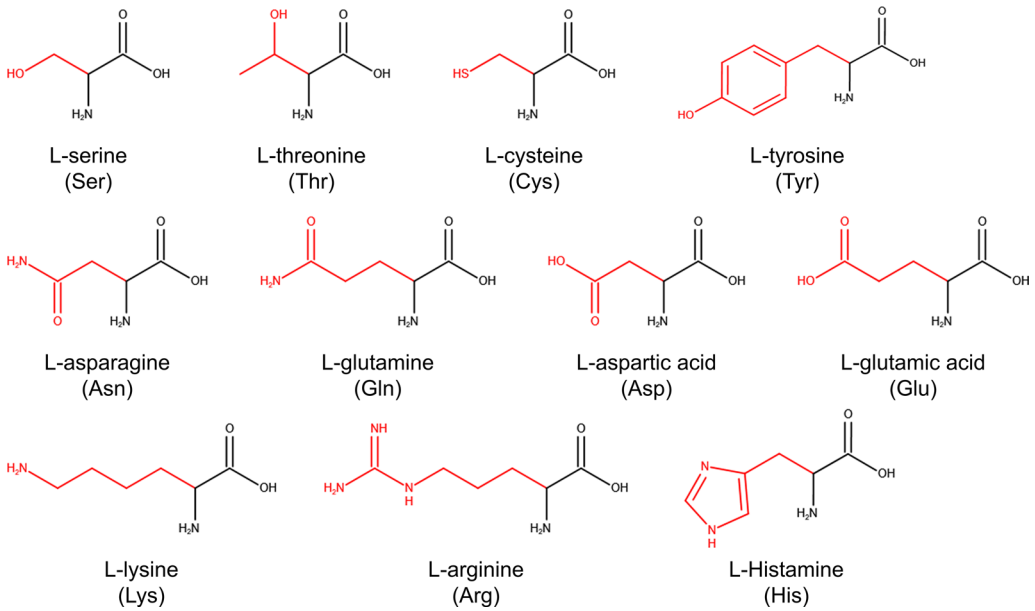

Fig. 1 Molecular structures of the 11 polar amino acids

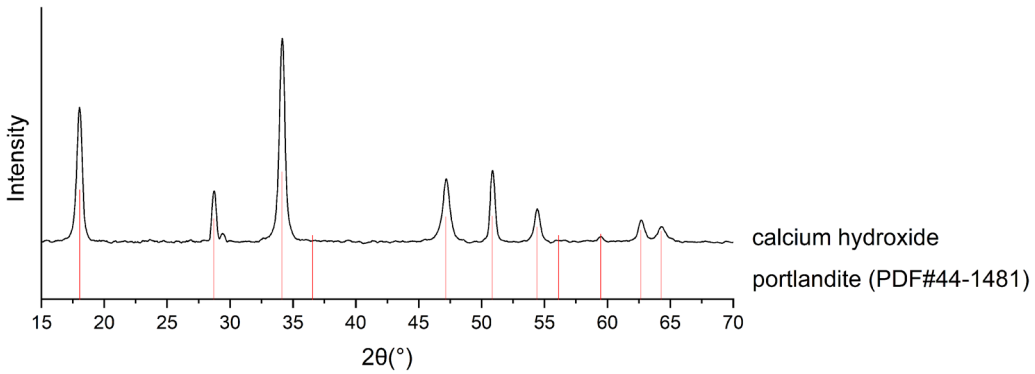

Fig. 2 X-ray diffraction pattern of calcium hydroxide

animal blood (~19% protein content [22]). The amino acid–water mixtures were then separately incorporated with calcium hydroxide and sand, at the ratio of calcium hydroxide: sand: distilled water = 1:3:1 by weight. Such ratios were chosen based on both ordinary material composition ratios in lime mortars and on preliminary tryouts performed on the materials. Additionally, a reference mortar specimen was prepared, with the composition of calcium hydroxide: sand: distilled water = 1:3:1 by weight. Altogether, 34 mortar mixtures were prepared 3 percentages for each of the 11 polar amino acids, plus 1 reference mortar. The fresh mortar mixtures were then transferred to petri dish molds and demolded after 5 days, and cured under laboratory condition (~25 °C, ~50% RH) until they were used for property tests (weight loss and surface hardness) and analyses (FTIR, XRD, TGA).

Methods

Within 30 days of curing, the weight loss and surface hardness of the specimens were measured after 2, 4, 6, 9, 16, 23 and 30 days of curing. After 30 and 180 days of curing, the specimens were ground to powder, passing through a 200-mesh (75 μm) sieve to sift out sand, so that the effects of amino acids solely on the lime binder can be evidenced. The sieved powder was then analyzed with Fourier transform infrared spectroscopy (FTIR), X-ray diffraction analysis (XRD), and thermogravimetric

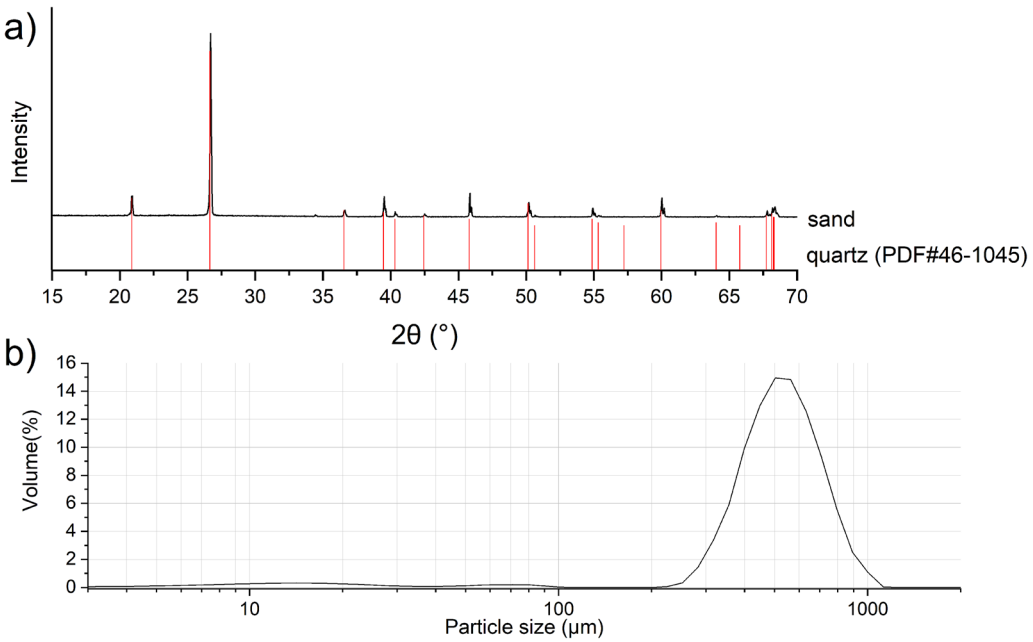

Fig. 3 **a** X-ray diffraction pattern and (**b**) particle size distribution curve of sand

analysis (TGA). Details of the tests and analyses performed are shown in Table 1.

Results

Weight loss and surface hardness

The hardening of lime mortars comprises two stages: water loss and setting. At the first stage (water loss), excess water is evaporated and/or absorbed by substrate, then starts the second stage (setting), in which both water loss and carbonation takes place, forming colloidal lime gel and gives mortar its initial strength [35]. Therefore, during lime mortar hardening, the mortar gradually loses water and starts gaining strength. Hence in this study, weight loss and surface hardness values were recorded. Both mortar weight loss and surface hardness values could reflect to which stage the setting has progressed, and at what rate the setting has progressed.

According to the weight loss results (Fig. 4 and Table 2), the reference mortar specimen achieved its highest weight loss value 18.90% on day 4, then slowly regained weight due to carbonation, and finally reached 17.54% on day 30. The surface hardness development of reference mortar showed similar patterns: the highest surface hardness increasing rate was achieved within 2 days of

Table 1 Details of the tests and analyses performed on mortar specimens

Test/analysis	Mortar curing time	Test device/analysis instrument	Test method/analysis working condition
Weight loss	2, 4, 6, 9, 16, 23 and 30 days	Electrical balance (accuracy 0.01 g, Shanghai Hochoice Apparatus Manufacturer Co. Ltd., China)	–
Surface hardness	2, 4, 6, 9, 16, 23 and 30 days	Shore D hardness durometer (Handpi Instruments, China)	Measurements were taken 5 times at different positions on specimen top surface, at least 6 mm apart, with the point of the indenter at least 9 mm from any edge
FTIR	30 and 180 days	Thermo Fisher Scientific Nicolet iS50 Spectrometer (Thermo Fischer Scientific Inc., U.S.A.)	Wavenumber 4000–400 cm^{-1}, resolution 4 cm^{-1}, 64 scans
XRD	30 and 180 days	PANalytical X'pert^3 Powder X-ray diffractometer (PANalytical, Netherlands)	Cu-Kα radiation (λ = 1.540598 Å), 2θ range 5–90°, step scan 0.01°, scan speed 10° min^{-1}, working voltage 40 kV, working current 100 mA
TGA	30 and 180 days	Mettler Toledo TGA/DSC1 instrument (Mettler Toledo, Switzerland)	Room temperature to 1000 °C, N_2 atmosphere, heating rate 10 °C min^{-1}

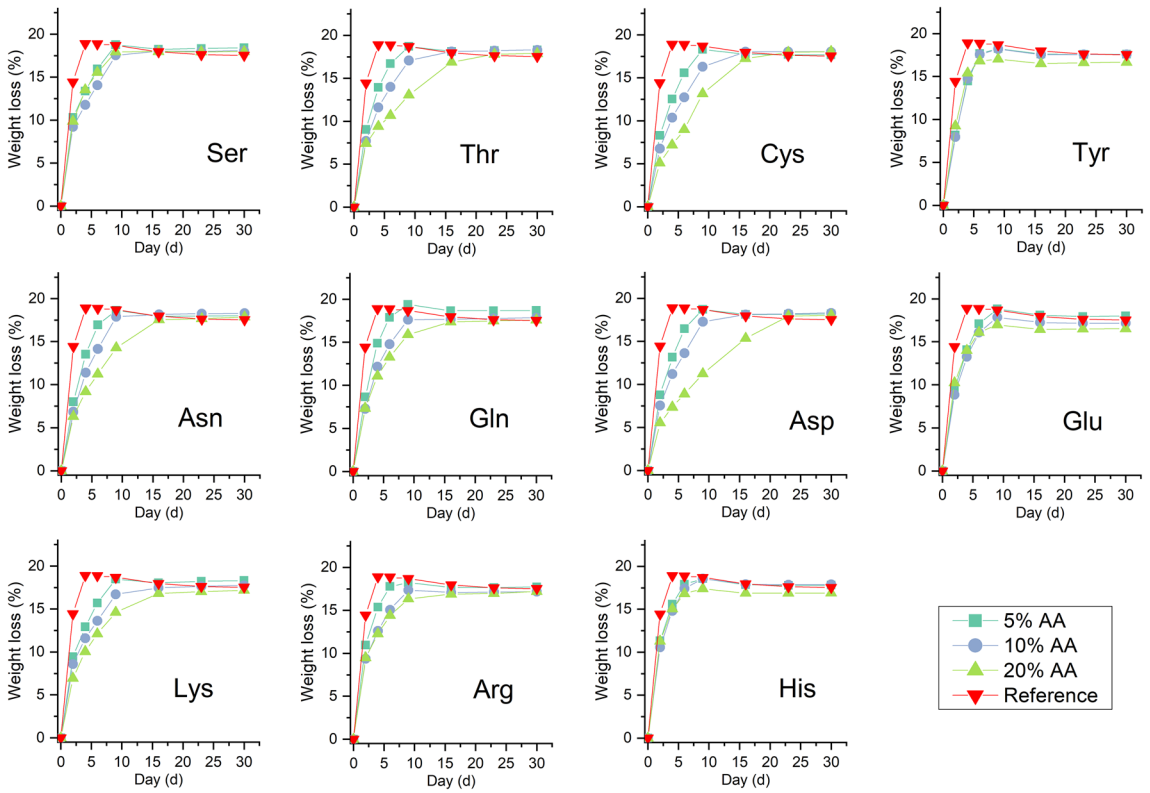

Fig. 4 Specimen weight loss values after 2, 4, 6, 9, 16, 23 and 30 days of curing

curing (surface hardness 22.2 ± 1.1 HD on day 2), then the hardness values slowly climbed up during the following 28 days and finally reached 38.0 ± 1.6 HD on day 30.

For specimens with amino acids addition, their highest weight loss values ranged from 16.96% (20% Glu) to 19.39% (5% Gln), which did not differ much from that of the reference mortar (18.90%). However, the time that it took for the mortars to reach their highest weight loss values was greatly delayed. According to Table 2, all mortars with amino acid addition took at least 9 days to reach their weight loss peaks, and some even didn't show any regained weight until day 30, indicating that the mortar drying process was significantly slowed down when compared with the reference mortar (weight loss peak on day 4). In addition, according to Fig. 4 and Table 2, the higher the amino acid concentration, the more evidenced was its slow-down effect on mortar drying.

Such result might be due to that polar amino acids are capable of forming H-bonds with water molecules [36], physically binding water so that it is not easily lost. It is therefore logical to deduce that the addition of polar amino acids into mortars could on one hand improve their water retention property, preventing water from quickly leaking off into porous substrates, yet on the other hand might delay mortar strength increase since excessive water is still present at the initial stage of mortar setting. This assumption was confirmed by the surface hardness results, since mortars with amino acid addition generally didn't achieve sufficiently high surface hardness until after 9 days of curing (Fig. 5), clearly showing delayed mortar strength increase caused by delayed mortar drying.

Additionally, the value difference between the highest weight loss and the weight loss value on day 30 could roughly reflect the degree of mortar carbonation. To be more specific, positive values (e.g., for reference mortar the value difference is 1.36%, see Table 2) suggest that until day 30, mortar weight gain values due to carbonation were higher than weight loss values due to water loss. It is shown in Table 2 that within 30 days of curing, not only all specimens with amino acid addition had lower value differences (the highest being 0.75% by the specimen 5% Glu), but their value differences also decreased with increased amino acid concentration. Such results indicated that the addition of amino acids into mortars could inhibit the carbonation process, and the more the amino acids were added, the more obvious were their inhibiting effects.

However, taking surface hardness results into consideration, such inhibiting effects on carbonation seemed to

Table 2 Highest weight loss of the specimens, mortar curing time at highest weight loss, and value difference between the highest weight loss and the weight loss on day 30

Specimen	Highest weight loss (%)	Mortar curing time at highest weight loss	Difference between highest weight loss and weight loss on day 30 (%)
Reference	18.9	4 d	1.36
5% Ser	18.78	9 d	0.35
10% Ser	18.08	30 d	0
20% Ser	17.98	30 d	0
5% Thr	18.71	9 d	0.4
10% Thr	18.31	30 d	0
20% Thr	17.88	30 d	0
5% Cys	18.3	9 d	0.63
10% Cys	18.05	16 d	0
20% Cys	18.04	30 d	0
5% Tyr	18.25	9 d	0.65
10% Tyr	18.2	9 d	0.64
20% Tyr	17.03	9 d	0.37
5% Asn	18.65	9 d	0.64
10% Asn	18.31	9 d	0
20% Asn	17.86	30 d	0
5% Gln	19.39	9 d	0.69
10% Gln	17.86	30 d	0
20% Gln	17.59	30 d	0
5% Asp	18.73	9 d	0.53
10% Asp	18.3	30 d	0
20% Asp	18.06	30 d	0
5% Glu	18.81	9d	0.79
10% Glu	17.85	9d	0.68
20% Glu	16.96	9d	0.43
5% Lys	18.47	9d	0.15
10% Lys	17.75	30 d	0
20% Lys	17.17	30 d	0
5% Arg	18.23	9d	0.51
10% Arg	17.36	9d	0.17
20% Arg	17.20	30 d	0
5% His	18.55	9d	0.75
10% His	18.55	9d	0.67
20% His	17.38	9d	0.5

promote long-term mortar strength development, since after 30 days of curing, nearly all mortars with amino acid addition showed increased surface hardness values with increasing amino acid concentration (Fig. 6). Eventually, all mortars with 20% amino acid addition achieved similarly high surface hardness values on day 30, ranging from 77.6 ± 1.1 HD by 20% His to 90.4 ± 1.0 HD by 20% Ser, which were significantly higher than that of the reference mortar (38.0 ± 1.6 HD).

Finally, it should be noted that a few specimens (e.g. 5% Thr, 10% Tyr, 5% Glu, 5% Arg and 5% His) showed decreased hardness values after 7 days of curing, and their standard deviation values were greater as well, which was caused by specimen surface cracking due to durometer indentation (Fig. 7). Thus, the surface hardness values obtained by the present study may not be accurate compared with standard property tests such as compressive strengths and flexural strengths which shall be conducted in future studies. However, surface hardness could still serve as a good indicator for mortar mechanical strengths, and reflect the general trends of effects exerted by amino acids.

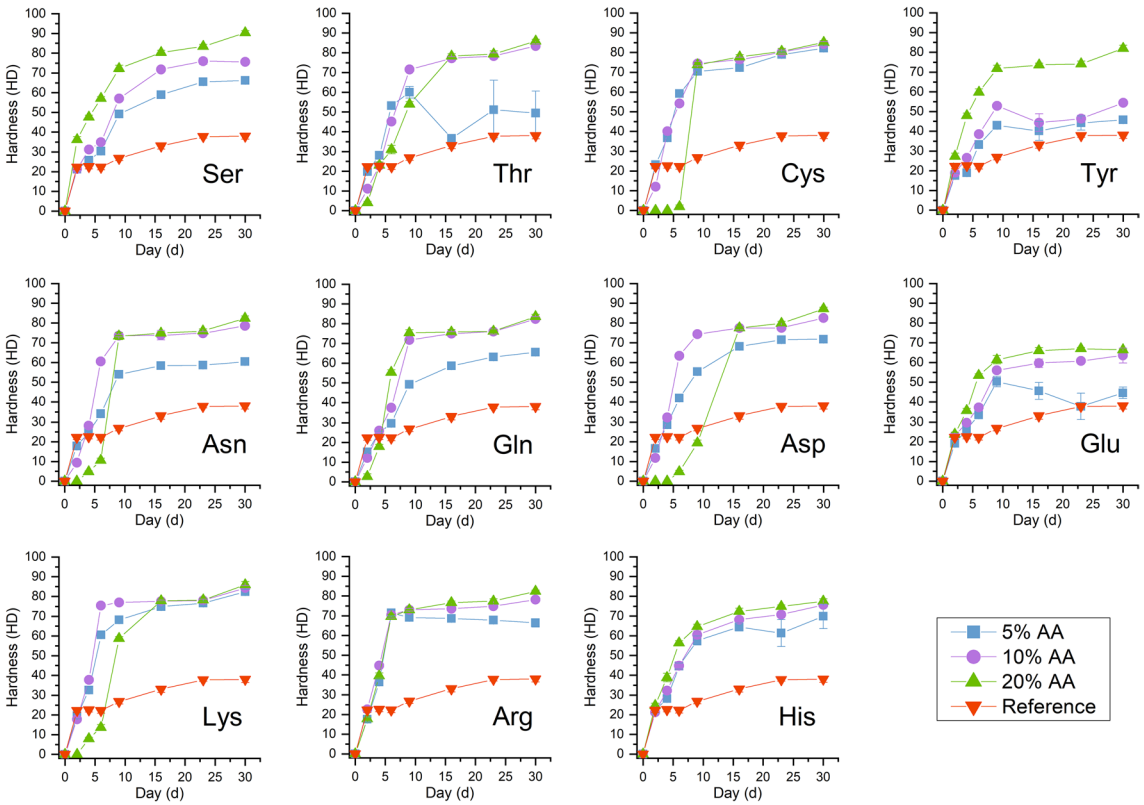

Fig. 5 Surface hardness values of mortar specimens after 2, 4, 6, 9, 16, 23 and 30 days of curing

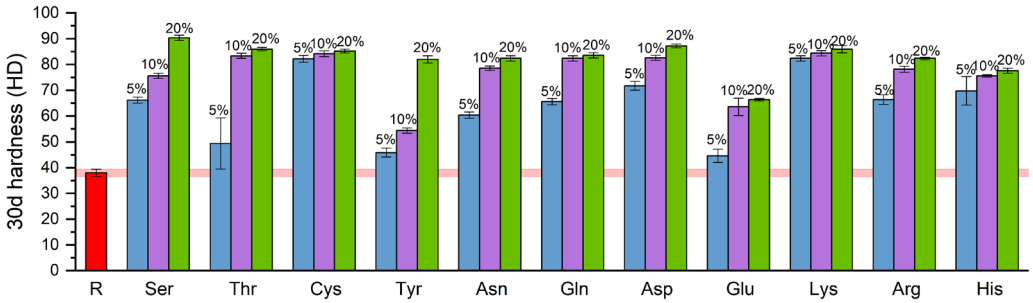

Fig. 6 Surface hardness values of mortar specimens after 30 days of curing

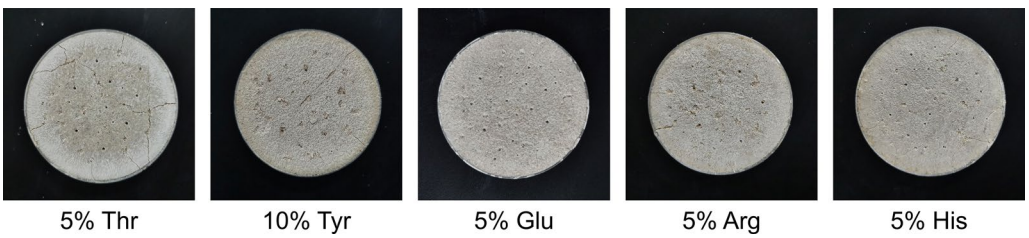

Fig. 7 Surface cracks of some mortar specimens (5% Thr, 10% Tyr, 5% Glu, 5% Arg and 5% His) after 7 days of curing, due to durometer indentation

FTIR

FTIR spectra (Fig. 8) showed that the major crystalline form of calcium carbonate in reference specimen (without amino acid) after 30 days of curing was calcite, which was evidenced by the circle symbols at band positions of 873 cm^{-1} (ν2) and 713 cm^{-1} (ν4). After 180 days of curing, however, apart from calcite, aragonite was additionally formed, as indicated by the diamond symbols at aragonite band positions of 858 cm^{-1} (ν2) and 700 cm^{-1} (ν4).

It is somewhat unexpected to find the new formation of aragonite after 180 days of curing, since usually calcite is the most common crystalline form under ambient curing conditions, and aragonite is favored under more extreme conditions, such as high temperatures [37, 38] and high pressures [39, 40]. According to Tai and Chen [37], under room temperature (24 °C), solution pH above 12 almost exclusively results in calcite formation, while under lower pH the major products were aragonite (pH 10.5–11.5, max at 11.0) and vaterite (pH 8.5–10.5, max at 9.5). Therefore, the difference between the calcium carbonate crystalline forms after 30 and 180 days of curing could be attributed to solution pH in mortar pores. When lime carbonation began, $Ca(OH)_2$ dissolved in pore water and formed saturated $Ca(OH)_2$ solution, whose initial pH around 12.5 under 25 °C lead to almost exclusive formation of calcite after 30 days of curing. After 180 days of curing, however, with the progress of carbonation, the continuous consumption of $Ca(OH)_2$ could eventually decrease the amount of available lime dissolved in pore solution, thus lowering solution pH and favored aragonite formation.

For specimens with amino acid addition, although the calcite ν2 band at ~ 873 cm^{-1} was present in all their spectra (Fig. 8), the ν4 band at 713 cm^{-1} was sometimes not evidently present. To be more specific, the ν4 band was present in specimens with Tyr, Glu and His at all percentages of addition (5%, 10% and 20%), and in specimens with Ser, Cys, Asn, Gln, Asp and Arg at lower percentages of addition (5%, or both 5% and 10%), but it was almost undistinguishable in all the other specimens, except for the "20% Ser" specimen, which showed a fairly strong band at 713 cm^{-1}. However, this could be due to overlapped band positions of calcite and the amino acid serine, since the band at 873 cm^{-1} was not proportionally strong. Therefore, whether calcite was present in 20% Ser specimen should be further validated by XRD results.

In addition, the high ν2/ν4 intensity ratio in the FTIR spectra indicates low crystallinity of the material, hence suggesting the presence of amorphous calcium carbonate (ACC) [41, 42] in some of the specimens with amino acid addition. The presence and the possible mechanism on ACC formation will be further discussed in the following sections.

XRD

Figure 9 showed the XRD patterns (2θ range 25.5–33.5°) of reference mortar specimen and specimens with amino acid addition after 30 and 180 days of curing. As described in Section "Methods", before analysis, the specimens were ground to powder, passing through a 200-mesh (75 μm) sieve to sift out sand, so that the XRD patterns can be simplified, showing primarily the peaks of the still uncarbonated lime [portlandite (101) peak at 2θ = 28.7° [43]] and the carbonation product calcium carbonate.

However, during the grinding-sieving process, sometimes sand was not completely excluded from the analyzed mortar powder, so some specimens with amino acid addition (e.g. Thr, Cys, Asp, Glu, Lys, Arg, His) also showed the main (101) quartz peak at 2θ = 26.7° [44] in their XRD patterns. It is interesting to note that the quartz peak appeared mostly in patterns of specimens with 20% amino acid addition. This could indicate a better binder-aggregate adhesion as a result of higher percentage organic additive addition, which made the separation between lime and sand difficult, hence the presence of quartz peaks in such specimens.

As for the reference specimen, XRD results confirmed the FTIR results on the major presence of calcite after 30 days of curing, and the additional presence of aragonite after 180 days of curing, which was evidenced by the circle symbols at the main (104) calcite peak of 2θ = 29.4° [45] on the "Ref 30d" XRD pattern, and by the diamond symbols at the aragonite peaks of 2θ = 26.2°, 27.3°and 33.1°, corresponding to (111), (021) and (012) crystallographic planes [46] on the "Ref 180d" XRD pattern.

The XRD results also corroborated with the FTIR results that calcite was present in the following specimens with amino acid addition: Tyr, Glu and His at all percentages, 5% Ser, 5% Cys, 5% Asn, 5% Gln, 5% and 10% Asp, 5% Arg. As for the other specimens, the very low main calcite peak at 2θ = 29.4°, together with the fact that no distinct presence of other crystalline calcium carbonate (i.e. aragonite, vaterite) peaks was found in their XRD patterns, confirmed again the FTIR results that amorphous calcium carbonate should be present. Moreover, the XRD pattern of 20% Ser specimen showed very low main calcite peak at 2θ = 29.4°, so the amount of crystalline calcite in the 20% Ser specimen should be low.

Therefore, both the FTIR and XRD results suggested that all amino acids displayed the ability of calcite inhibition and ACC facilitation, with Thr and Lys performing the best (i.e., they could almost completely stabilize ACC at all 3 percentages investigated by the

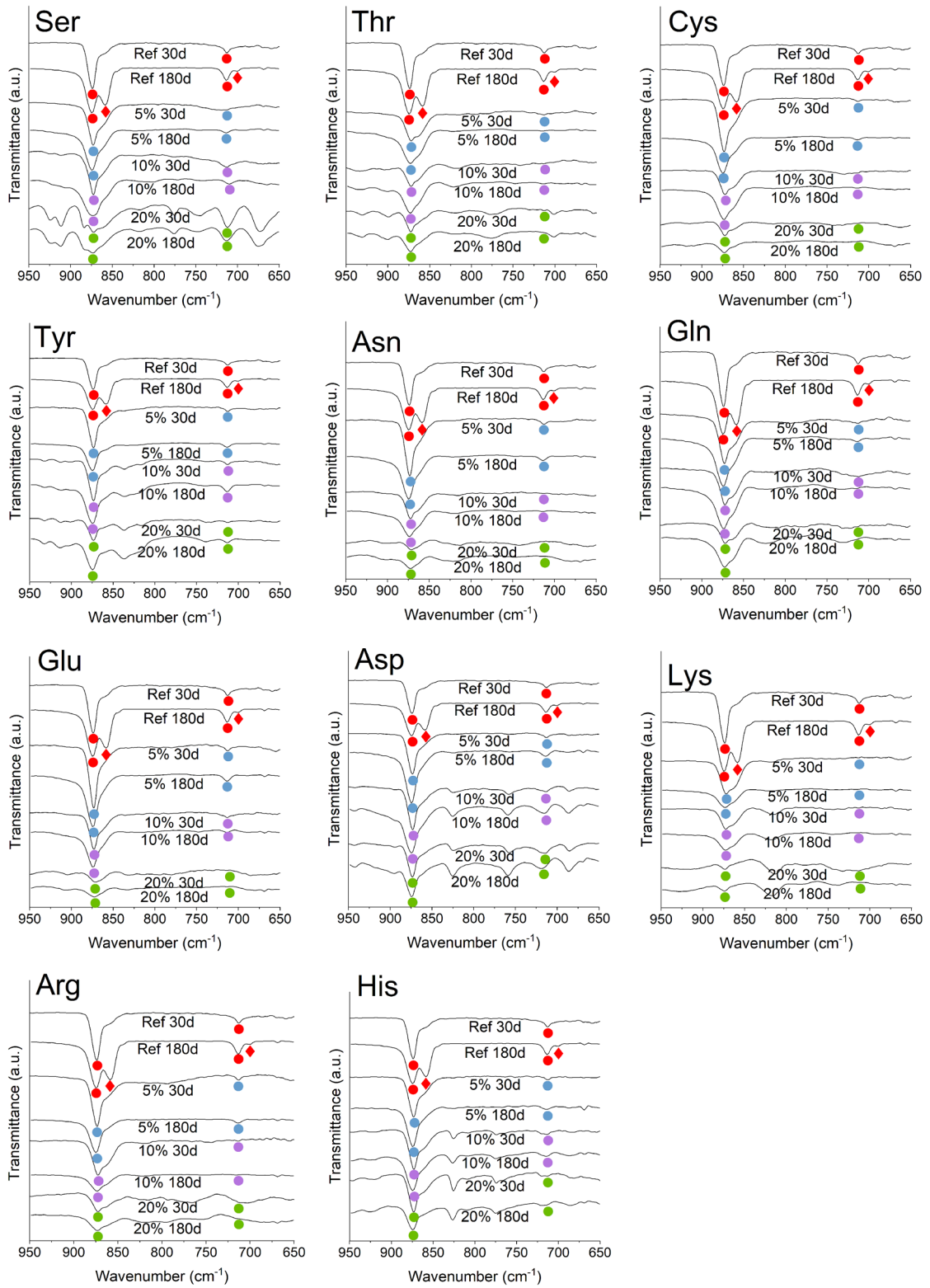

Fig. 8 FTIR spectra (wavenumber range 950–650 cm^{-1}) of reference mortar specimen (Ref) and specimens with amino acid addition after 30 and 180 days (d) of curing. Circle symbols (●): characteristic calcite absorption bands at 873 cm^{-1} (v2) and 713 cm^{-1} (v4); diamond symbols (♦): characteristic aragonite absorption bands at 858 cm^{-1} (v2) and 700 cm^{-1} (v4)

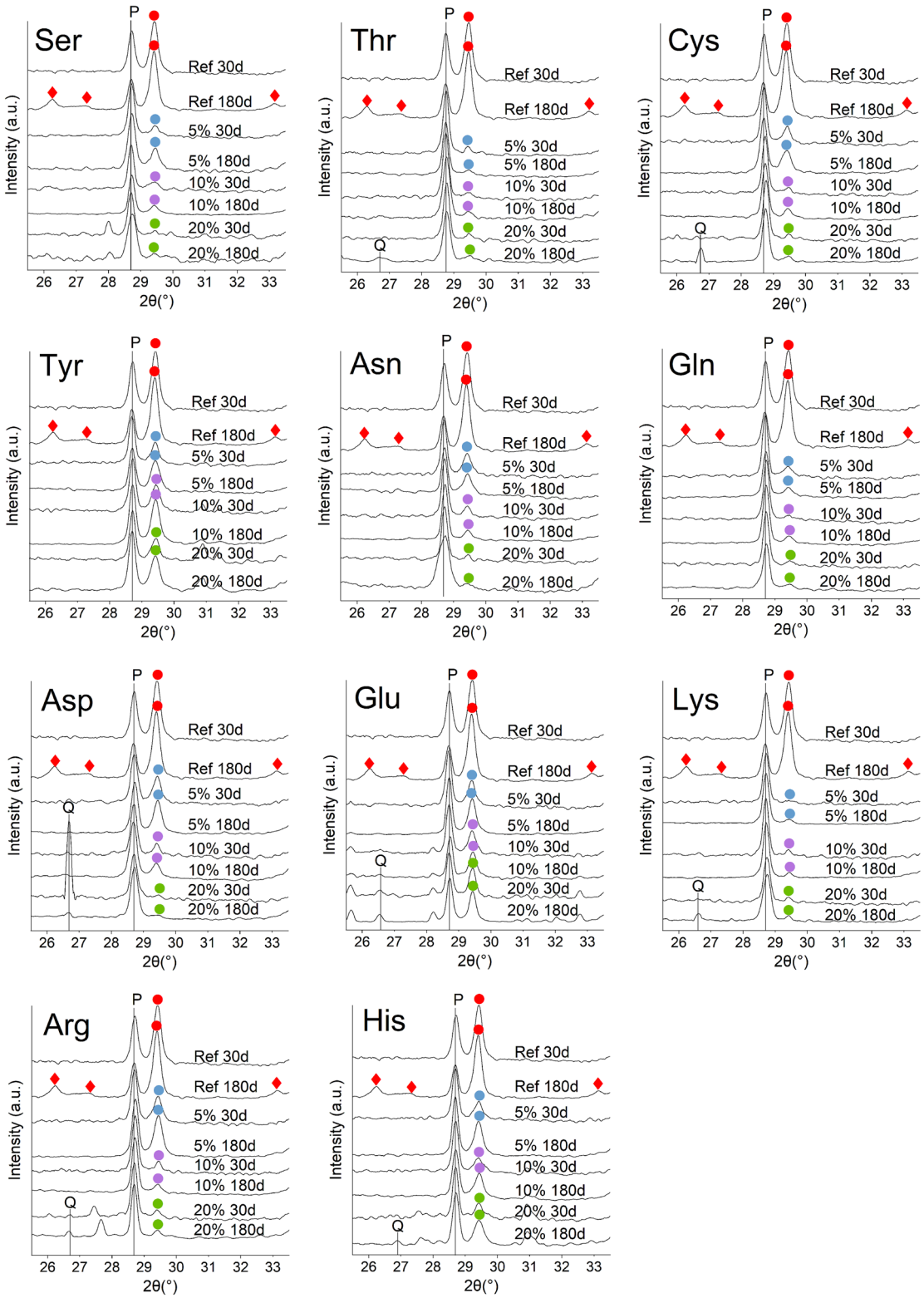

Fig. 9 XRD patterns (2θ range 25.5–33.5°) of reference mortar specimen (Ref) and specimens with amino acid addition after 30 and 180 days (d) of curing. Circle symbols (●): characteristic calcite diffraction peaks at 2θ = 29.4° (104); diamond symbols (♦): characteristic aragonite diffraction peaks at 2θ = 26.2° (111), 27.3° (021) and 33.1° (012); P: portlandite from uncarbonated lime; Q: quartz resulted from residual sand after sieving

present study), Tyr, Glu and His performing the worst (since calcite was present at all 3 percentages of addition), and for the remaining 6 amino acids (Ser, Cys, Asn, Gln, Asp and Arg), with the increase of amino acid concentration, the capability of calcite inhibition and ACC facilitation seemed to become greater.

Additionally, the XRD patterns revealed that in some of the specimens where calcite was present (Tyr, Glu and His at all percentages, 5% Ser, 5% Cys, 5% and 10% Asp, 5% Arg), compared with the intensity of the calcite peak at $2\theta = 29.4^{\circ}$ after 30 days of curing, the peak intensity increased after 180 days of curing. The newly formed calcite in the specimens could derive from two sources: formation of new calcite from recently carbonated lime and/or transformation from previously existing ACC to calcite.

TGA

Table 3 and Fig. 10 respectively showed weight loss of the 11 polar amino acids and the specimens within 550–750 °C by thermogravimetric analysis, in order to evaluate the carbonation degree of lime mortars. For the reference specimen, the weight loss within this temperature range corresponds to decomposition of calcium carbonate; for specimens with amino acid addition, the weight loss within 550–750 °C was in part due to $CaCO_3$ decomposition, and in part due to amino acid residues.

For the amino acids, their weight loss values within 550–750 °C fell between 0.53–10.86% (Table 3), with Thr at the lowest, and His at the highest. Since the 10.86% weight loss seems high, it is necessary to calculate the approximate contribution of the amino acid histamine at its highest concentration (20% by weight) into mortars.

Table 3 Thermal weight loss (%) of the 11 polar amino acids within 550–750 °C

	Ser	Thr	Cys	Tyr	Asn	Gln	Asp	Glu	Lys	Arg	His
550–750 °C thermal weight loss (%)	2.25	0.53	0.89	2.74	5.81	3.9	4.39	2.6	0.56	3.58	10.86

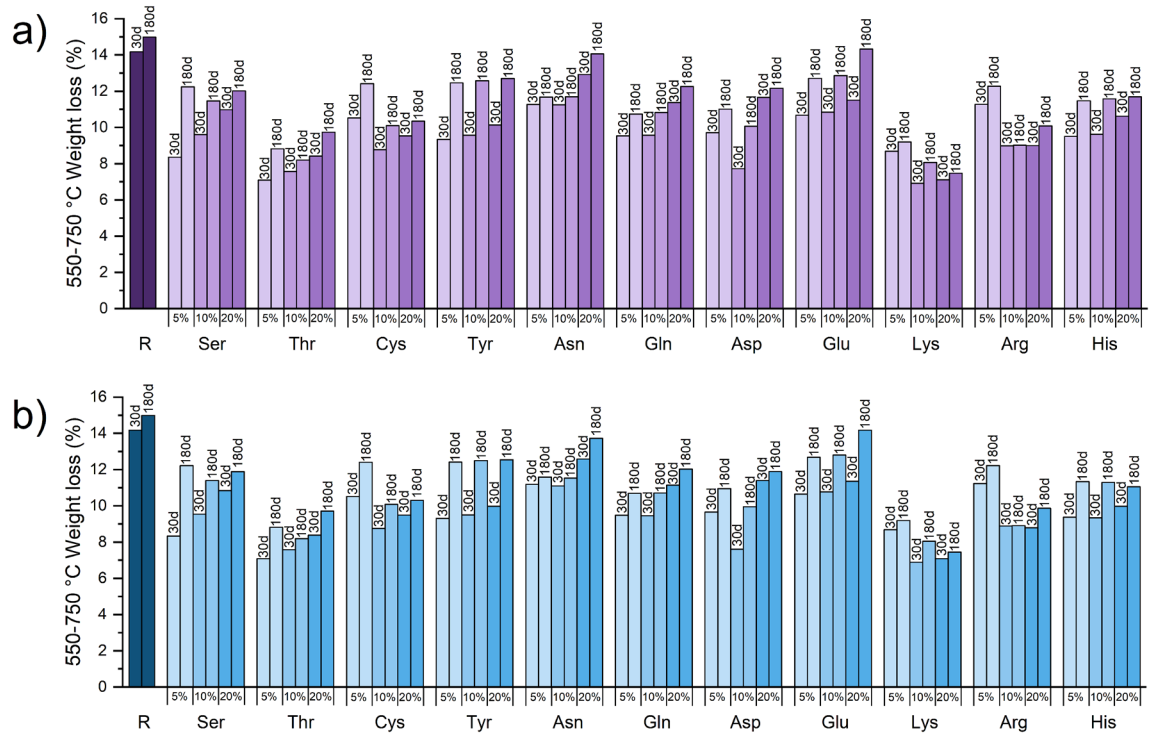

Fig. 10 Thermal weight loss (within 550–750 °C) of reference mortar specimen (R) and specimens with amino acid addition after 30 and 180 days (d) of curing. **a** original thermal weight loss values; (**b**) recalculated thermal weight loss values within 550–750 °C, subtracting theoretical weight loss from amino acids

As described in Section "Mortar specimen preparation", the amino acids (AA) were added in distilled water (W) at AA/ (AA + W) = 5, 10 and 20%-w/w. Hence for 20% amino acid addition, AA: W = 0.25:1-w/w. In mortars, the ratio of calcium hydroxide: sand: distilled water was 1:3:1 by weight. Hypothesizing that all water evaporated during mortar curing, the solid content of 20% amino acid addition in mortar was AA: (AA + calcium hydroxide + sand) = 0.25/(0.25 + 1 + 3) ≈ 5.88%. Therefore, the approximate contribution of 20% His to mortar within 550–750 °C is 5.88% × 10.86% ≈ 0.64%; similarly, the contribution values of 5% and 10% His addition to mortar are 0.14% and 0.29%, respectively.

Figure 10b showed recalculated thermal weight loss values, subtracting theoretical weight loss from amino acids. According to Fig. 10b, the thermal weight loss values within 550–750 °C of specimens with amino acid addition after 30 days of curing were 6.90% (10% Lys) to 12.58% (20% Asn), and the weight loss values after 180 days of curing were 7.45% (20% Lys) to 14.17% (20% Glu), which were all lower than the values of reference specimen (14.17 and 14.99%). Therefore, the addition of amino acid could slow down lime carbonation process and decrease mortar's carbonation degree, corroborating the results from Section "Weight loss and surface hardness".

Such result may further explain another issue: aragonite was additionally formed after 180 days of curing in reference mortar without amino acid, while no distinct presence of aragonite was found in any specimen with amino acid addition. As aforementioned, the formation of aragonite in reference mortar could be due to reduced alkalinity in pore solution as a result of lime consumption. In the case of mortars with amino acid, lime consumption was hindered, so the mortar was able to maintain its relatively high alkalinity, and consequently precipitate calcite as the major product.

It should again be noted that after 180 days of curing, the lowest weight loss values within 550–750 °C among all specimens were achieved by specimens with Thr (8.19–9.71%) and Lys (7.45–9.19%) addition (Fig. 10b). According to FTIR and XRD results (Section "FTIR" and "XRD"), Thr and Lys when added in lime mortars, seemed to form the least amount of calcite. Now taking into the TGA results into consideration, the low intensity of calcite FTIR bands and XRD peaks of specimens with Thr and Lys addition was not only due to the formation of amorphous calcium carbonate as major carbonation product, but also due to the diminished carbonation degree of these mortars, possibly because amino acids could on one hand increase solution viscosity and limit ion diffusion, and on the other hand adsorb onto $Ca(OH)_2$ particle surface [47, 48], further preventing lime carbonation. However, it is not clear why Thr and Lys seem to have the greatest ability in retarding the carbonation process of lime mortars.

Discussion

The results of the present study suggested that the addition of polar amino acids into mortars could delay mortar drying and inhibit carbonation process, and the higher the amino acid concentration, the more evidenced was its slow-down effect on mortar drying and mortar strength increase, as well as the inhibiting effect on mortar carbonation. However, such inhibiting effects seemed to promote mortar strength development in the long term, and generally the higher the amino acid concentration, the higher the mortar surface hardness values. Subsequent analyses detected the presence of amorphous calcium carbonate (ACC) in mortars with amino acid addition, and the formation of ACC could increase mortar strength, as mentioned by some studies [49, 50] that ACC phases frequently function as mechanical stiffener in biomineralization.

Fourier transform infrared spectroscopy (FTIR), X-ray diffraction (XRD) and thermogravimetry (TGA) analysis results suggested that all amino acids displayed the ability of calcite inhibition and amorphous calcium carbonate (ACC) facilitation, but to different degrees. It is intriguing to note that the effect revealed by a single amino acid can be similar to that of whole proteins, since in our previous studies on lime-based mortars with oxblood addition, the formation of ACC in mortars with oxblood addition was also confirmed by FTIR, XRD, TG-DSC and SEM analyses [12, 51, 52]. It was speculated in these previous studies that ACC stabilization could be realized through lowered supersaturation in solution by combination between calcium ions and protein sections rich in glutamic acid, serine, glycine, and carbohydrates. The results of the present study demonstrated that, rather than Asp, Glu and Ser which were conventional ACC stabilizers [34, 48, 53], Thr and Lys seemed to demonstrate the greatest capability in ACC stabilization, which was quite a surprise.

Most studies on ACC stabilization via amino acids focused on the effects of acidic amino acids (i.e. Asp and Glu), especially Asp. According to these studies, Asp is able to stabilize a dense liquid phase of calcium carbonate even before the formation of ACC [54–57], and upon delayed precipitation of ACC, Asp can also stabilize it [48, 53] and increase its lifetime [48]. The possible explanation for such stabilization was that the negatively charged carboxylate groups could sequester calcium from solution to inhibit the precipitation of a solid phase [55].

However, most of these previous studies were conducted at pH values close to 7, which is the common biological and physiological condition, and quite different from the highly alkaline pH environment created by lime (pH usually above 12) in our study. Under pH≈7, Asp and Glu are negatively charged amino acids, Lys, Arg and His are positively charged, while the remaining amino acids are non-charged. However, under pH≈12, Cys, Asp, Glu and Tyr can be classified as negatively charged amino acids, while Ser, Thr, Cys, Asn, Gln, Lys, Arg and His are non-charged polar ones with hydrogen bond donor side chain groups [58, 59].

Picker et al. [59] investigated the specific adsorption of amino acids on C–S–H, and assumed that at pH < 11, the adsorption of amino acids on C–S–H is mainly dominated by and driven by electrostatic interactions between negatively charged amino acids (Asp, Glu, Tyr) and Ca^{2+} ions; yet at pH ≥ 12, the binding of non-charged amino acids via H-bonds (e.g. Arg, Lys, Ser) and additional Ca^{2+} mediated adsorption (e.g. Asn with the amide group bearing a partial negative charge on the carbonyl oxygen) is favored. The results of our study generally concord with such assumption.

In the present study, the ability of polar amino acids to stabilize ACC can be estimated by the amount of calcite formed in the specimens through the main calcite peak intensity at 2θ = 29.4° in the XRD patterns lower calcite peak intensity could indicate better ACC stabilization. According to XRD results (Fig. 9) and molecular structures of the polar amino acids (Fig. 1), the non-charged H-donating amino acids (Ser, Thr, Cys, Lys, Arg) and the amino acids with amide functions (Asn, Gln) indeed showed greater ACC stabilization than negatively charged Cys, Asp, Glu and Tyr.

The only exception was His, which as a H-donating amino acid didn't seem to stabilize ACC. According to Bentov et al. [60], stable ACC formation is possibly induced by amino acids which are strongly bound to the mineral phase, and the energy required for this bond dissociation raises the energy barriers between ACC and crystalline phases thus kinetically slowing down the crystallization of the ACC. This may explain the insufficient ability of His on ACC stabilization: as displayed in Fig. 1, histamine has a rigid and bulky imidazole ring on its side chain, which would hinder its incorporation into calcium carbonate [61]. In addition, the capability of Thr and Lys on ACC promotion seem to be the best, which still calls for further research on their interaction mechanisms.

Conclusions

The present study intends to explore the possible mechanism of traditional mortars with protein additives by first studying the influence of polar amino acids on the carbonation of lime mortars. Some preliminary results were obtained, and showed that within 30 days of mortar curing, the weight evolution and surface hardness values were monitored, and after 30 and 180 days of curing, the specimens were analyzed with Fourier transform infrared spectroscopy (FTIR), X-ray diffraction (XRD) and thermogravimetry (TGA). The following conclusions may be drawn:

1. Within 30 days of curing, the weight loss results of the specimens demonstrated that the addition of polar amino acids into mortars could delay mortar drying and inhibit carbonation process. Moreover, the higher the amino acid concentration, the more evidenced was its slow-down effect on mortar drying, as well as the inhibiting effect on mortar carbonation.
2. After 30 days of curing, mortars with amino acid addition displayed higher surface hardness values than the reference specimen, and increasing surface hardness values were achieved with increasing amino acid concentration. Within the curing process, the addition of amino acids caused retarded setting, which should be again caused by the slow drying of these specimens.
3. In respect to the reference specimen, all specimens with amino acid addition showed higher ν2/ν4 calcite band intensity ratio in their FTIR spectra, together with lower main calcite peak intensity in their XRD patterns, suggesting that all amino acids displayed the ability of calcite inhibition and ACC facilitation, with Thr and Lys performing the best, Tyr, Glu and His performing the worst, and for the remaining 6 amino acids (Ser, Cys, Asn, Gln, Asp and Arg), with the increase of the of amino acid concentration, the capability of calcite inhibition and ACC facilitation seemed to become greater.
4. Through the weight loss within 550–750 °C which primarily represents decomposition of calcium carbonate, thermal analysis results showed that the addition of amino acid could greatly slow down lime carbonation process and decrease mortar's carbonation degree.

Most previous studies on the control of amino acids over calcium carbonate were conducted at pH values close to 7, which is the common biological and physiological condition; while the present study was conducted in rather highly alkaline pH environment created by lime mortar (pH usually above 12). Under such high pH, the binding of non-charged amino acids via H-bonds (e.g. Ser, Thr, Cys, Lys, Arg) and additional Ca^{2+} mediated adsorption (e.g. Asn and Gln with the amide group

bearing a partial negative charge on the carbonyl oxygen) may be favored. However, it still remains elusive as to why Thr and Lys seemed to have the greatest capability on ACC stabilization and calcite inhibition, which requires further study on such issue.

Acknowledgements
Not applicable.

Author contributions
KZ designed the methodology and experiment, performed data analysis, and wrote the original draft. YZ conducted the experiment and executed data analysis. LW, LH and TD helped with data methodology and interpretation. FY and YL conceptualized this research and primarily reviewed and edited the manuscript. YZ helped reviewing and editing the manuscript. All authors read and approved the final manuscript.

Funding
This work was supported by the National Natural Science Foundation of China [Grant Numbers 52108031; B0501 21975202]; Key R & D program in Shaanxi Province [Grant Number 2020SF-363]; Education Department of Shaanxi Provincial Government [Grant Number 21JK0385].

Availability of data and materials
The datasets used and/or analysed during the current study are available from the corresponding author on reasonable request.

Declarations

Competing interests
The authors declare that they have no competing interests.

Author details
[1]China-Central Asia "the Belt and Road" Joint Laboratory On Human and Environment Research, Key Laboratory of Cultural Heritage Research and Conservation, School of Culture Heritage, Northwest University, Xi'an 710127, China. [2]Northwest University Museum, Xi'an 710068, China.

Received: 8 September 2022 Accepted: 11 November 2022
Published online: 23 November 2022

References

1. Zhao P, Li G, Zhang Y. Understanding and assessment of ancient Chinese pig blood-lime mortar. Adv Mater Res. 2014;997:446–9.
2. Owen T. The fourteen books of Palladius Rutilius Taurus Æmilianus, on agriculture. 1st ed. London: J. White; 1807.
3. Brun G. The transmission and circulation of practical knowledge on art and architecture in the middle ages. Milan: Politecnico di Milano; 2015.
4. Hawthorne JG, Cyril SS. Theophilus on divers arts. 1st ed. New York: Dover Publications; 1979.
5. Neve R. The city and country purchaser's and builder's dictionary. 1st edn. London: A. M. Kelley; 1726.
6. Thornton J. A brief history and review of the early practice and materials of gap-filling in the west. JAIC. 1998;37(1):3–22.
7. Pahlavan P, Manzi S, Sansonetti A, Bignozzi MC. Valorization of organic additions in restorative lime mortars: spent cooking oil and albumen. Constr Build Mater. 2018;181:650–8.
8. Falkjar K. An experimental study on the effects of casein protein in unreinforced lime mortar specimens. Ottawa: Carleton University; 2019.
9. Fang S, Zhang K, Zhang H, Zhang B. A study of traditional blood lime mortar for restoration of ancient buildings. Cem Concr Res. 2015;76:232–41.
10. Zhang K, Wang L, Tie F, Yang F, Liu Y, Zhang Y. A preliminary study on the characteristics of lime-based mortars with egg white addition. Int J Archit Herit. 2022;16(8):1184–98.
11. Ventolà L, Vendrell M, Giraldez P, Merino L. Traditional organic additives improve lime mortars: new old materials for restoration and building natural stone fabrics. Constr Build Mater. 2011;25(8):3313–8.
12. Zhang K, Corti C, Grimoldi A, Rampazzi L, Sansonetti A. Application of different fourier transform infrared (FT-IR) methods in the characterization of lime-based mortars with oxblood. Appl Spectrosc. 2019;73(5):479–91.
13. Centauro I, Cantisani E, Grandin C, Salvini A, Vettori S. The influence of natural organic materials on the properties of traditional lime-based mortars. Int J Archit Herit. 2017;11(5):670–84.
14. Elert K, Sánchez R, Benavides-Reyes C, Ordóñez F. Influence of animal glue on mineralogy, strength and weathering resistance of lime plasters. Constr Build Mater. 2019;226:625–35.
15. Alonso E, Martinez-Gomez L, Martinez W, Castano VM. Preparation and characterisation of ancient-like masonry mortars. Adv Compos Lett. 2002;11(1):33–6.
16. Zhao P, Jackson M, Zhang Y, Li G, Monteiro P, Yang L. Material characteristics of ancient Chinese lime binder and experimental reproductions with organic admixtures. Constr Build Mater. 2015;84:477–88.
17. Mydin O. Preliminary studies on the development of lime-based mortar with added egg white. Int J Technol. 2017;8(5):800–10.
18. Ng-Kwai-Hang KF, Hayes JF, Moxley JE, Monardes HG. Environmental influences on protein content and composition of bovine milk. J Dairy Sci. 1982;65(10):1993–8.
19. Almquist HJ, Lorenz FW. The solids content of egg white. Pout Sci. 1933;12(2):83–9.
20. Mine Y. Recent advances in the understanding of egg white protein functionality. Trends Food Sci Technol. 1995;6(7):225–32.
21. Vadehra D, Nath K, Forsythe R. Eggs as a source of protein. Cri Rev Food Sci Nutr. 1973;4(2):193–309.
22. Duarte RT, Carvalho Simões MC, Sgarbieri VC. Bovine blood components: fractionation, composition, and nutritive value. J Agric Food Chem. 1999;47(1):231–6.
23. Shen X, Belcher AM, Hansma PK, Stucky GD, Morse DE. Molecular cloning and characterization of lustrin A, a matrix protein from shell and pearl nacre of Haliotis rufescens. J Biol Chem. 1997;272(51):32472–81.
24. Levi Y, Albeck S, Brack A, Weiner S, Addadi L. Control over aragonite crystal nucleation and growth: an in vitro study of biomineralization. Chem Eur J. 1998;4(3):389–96.
25. Weiner S, Hood L. Soluble protein of the organic matrix of mollusk shells: a potential template for shell formation. Science. 1975;190(4218):987–9.
26. Suzuki M, Saruwatari K, Kogure T, Yamamoto Y, Nishimura T, Kato T, et al. An acidic matrix protein, Pif, is a key macromolecule for nacre formation. Science. 2009;325(5946):1388–90.
27. Addadi L, Moradian J, Shay E, Maroudas N, Weiner S. A chemical model for the cooperation of sulfates and carboxylates in calcite crystal nucleation: relevance to biomineralization. PNAS. 1987;84(9):2732–6.
28. Weiner S. Mollusk shell formation: isolation of two organic matrix proteins associated with calcite deposition in the bivalve Mytilus californianus. Biochemistry. 1983;22(17):4139–45.
29. Miyamoto H, Miyashita T, Okushima M, Nakano S, Morita T, Matsushiro A. A carbonic anhydrase from the nacreous layer in oyster pearls. PNAS. 1996;93(18):9657–60.
30. Khan RI, Ashraf W, Olek J. Amino acids as performance-controlling additives in carbonation-activated cementitious materials. Cem Concr Res. 2021;147: 106501.
31. Wolf SE, Loges N, Mathiasch B, Panthöfer M, Mey I, Janshoff A, et al. Phase selection of calcium carbonate through the chirality of adsorbed amino acids. Angew Chem Int Ed. 2007;46(29):5618–23.
32. Hazen RM, Filley TR, Goodfriend GA. Selective adsorption of L-and D-amino acids on calcite: Implications for biochemical homochirality. PNAS. 2001;98(10):5487–90.
33. Viedma C. Enantiomeric crystallization from DL-aspartic and DL-glutamic acids: implications for biomolecular chirality in the origin of life. Orig Life Evol Biosph. 2001;31(6):501–9.
34. Picker A, Kellermeier M, Seto J, Gebauer D, Cölfen H. The multiple effects of amino acids on the early stages of calcium carbonate crystallization. Z Krist Cryst Mater. 2012;227(11):744–57.
35. Cechova E. The effect of linseed oil on the properties of lime-based restoration mortars. Bologna: University of Bologna; 2009.
36. Hernández B, Pflüger F, Adenier A, Nsangou M, Kruglik SG, Ghomi M. Energy maps, side chain conformational flexibility, and vibrational

features of polar amino acids L-serine and L-threonine in aqueous environment. J Chem Phys. 2011;135(5):08B601.
37. Tai CY, Chen FB. Polymorphism of $CaCO_3$, precipitated in a constant-composition environment. AlChE J. 1998;44(8):1790–8.
38. Wray JL, Daniels F. Precipitation of calcite and aragonite. J Am Chem Soc. 1957;79(9):2031–4.
39. Jamieson JC. Phase equilibrium in the system calcite-aragonite. J Chem Phys. 1953;21(8):1385–90.
40. MacDonald GJ. Experimental determination of calcite-aragonite equilibrium relations at elevated temperatures and pressures. Am Mineral. 1956;41(9–10):744–56.
41. Beniash E, Aizenberg J, Addadi L, Weiner S. Amorphous calcium carbonate transforms into calcite during sea urchin larval spicule growth. Proc R Soc Lond. 1997;264(1380):461–5.
42. Gueta R, Natan A, Addadi L, Weiner S, Refson K, Kronik L. Local atomic order and infrared spectra of biogenic calcite. Angew Chem Int Ed. 2007;46(1–2):291–4.
43. Otero J, Starinieri V, Charola AE. Nanolime for the consolidation of lime mortars: a comparison of three available products. Constr Build Mater. 2018;181:394–407.
44. Buckley P, Hargreaves N, Cooper S. Nucleation of quartz under ambient conditions. Commun Chem. 2018;1(1):1–10.
45. Cizer Ö, Van Balen K, Elsen J, Van Gemert D. Carbonation reaction kinetics of lime binders measured using XRD 2nd International conference on accelerated carbonation for environmental and materials engineering. Rome: University of Rome; 2008.
46. Nassif N, Gehrke N, Pinna N, Shirshova N, Tauer K, Antonietti M, et al. Synthesis of stable aragonite superstructures by a biomimetic crystallization pathway. Angew Chem Int Ed. 2005;44(37):6004–9.
47. Orme CA, Noy A, Wierzbicki A, McBride MT, Grantham M, Teng HH, et al. Formation of chiral morphologies through selective binding of amino acids to calcite surface steps. Nature. 2001;411(6839):775–9.
48. Tobler D, Blanco R, Dideriksen K, Sand K, Bovet N, Benning L, et al. The effect of aspartic acid and glycine on amorphous calcium carbonate (ACC) structure, stability and crystallization. Procedia Earth Planet Sci. 2014;10:143–8.
49. Becker A, Ziegler A, Epple M. The mineral phase in the cuticles of two species of Crustacea consists of magnesium calcite, amorphous calcium carbonate, and amorphous calcium phosphate. Dalton Trans. 2005;10:1814–20.
50. Cartwright JH, Checa AG, Gale JD, Gebauer D, Sainz-Díaz CI. Calcium carbonate polyamorphism and its role in biomineralization: how many amorphous calcium carbonates are there? Angew Chem Int Ed. 2012;51(48):11960–70.
51. Zhang K, Grimoldi A, Rampazzi L, Sansonetti A, Corti C. Contribution of thermal analysis in the characterization of lime-based mortars with oxblood addition. Thermochim Acta. 2019;678: 178303.
52. Zhang K, Rampazzi L, Riccardi MP, Sansonetti A, Grimoldi A. Mortar mixes with oxblood: historical background, model sample recipes and properties. ADGEO. 2018;45:19–24.
53. Raiteri P, Demichelis R, Gale JD, Kellermeier M, Gebauer D, Quigley D, et al. Exploring the influence of organic species on pre-and post-nucleation calcium carbonate. Faraday Discuss. 2012;159(1):61–85.
54. Finney AR, Innocenti Malini R, Freeman CL, Harding JH. Amino acid and oligopeptide effects on calcium carbonate solutions. Cryst Growth Des. 2020;20(5):3077–92.
55. Bewernitz MA, Gebauer D, Long J, Cölfen H, Gower LB. A metastable liquid precursor phase of calcium carbonate and its interactions with polyaspartate. Faraday Discuss. 2012;159(1):291–312.
56. Evans D, Webb P, Penkman K, Kröger R, Allison N. The characteristics and biological relevance of inorganic amorphous calcium carbonate (ACC) precipitated from seawater. Cryst Growth Des. 2019;19(8):4300–13.
57. Sebastiani F, Wolf SL, Born B, Luong TQ, Cölfen H, Gebauer D, et al. Water dynamics from THz spectroscopy reveal the locus of a liquid–liquid binodal limit in aqueous CaCO3 solutions. Angew Chem Int Ed. 2017;56(2):490–5.
58. Štajner L, Kontrec J, Džakula B, Maltar-Strmečki N, Plodinec M, Lyons D, et al. The effect of different amino acids on spontaneous precipitation of calcium carbonate polymorphs. J Cryst Growth. 2018;486:71–81.
59. Picker A, Nicoleau L, Nonat A, Labbez C, Cölfen H. Identification of binding peptides on calcium silicate hydrate: a novel view on cement additives. Adv Mater. 2014;26(7):1135–40.
60. Bentov S, Weil S, Glazer L, Sagi A, Berman A. Stabilization of amorphous calcium carbonate by phosphate rich organic matrix proteins and by single phosphoamino acids. J Struct Biol. 2010;171(2):207–15.
61. Borukhin S, Bloch L, Radlauer T, Hill A, Fitch A, Pokroy B. Screening the incorporation of amino acids into an inorganic crystalline host: the case of calcite. Adv Funct Mater. 2012;22(20):4216–24.

Publisher's Note